Contents lists available at ScienceDirect

Stem Cell Research

journal homepage: www.elsevier.com/locate/scr

Short report

Generation of human induced pluripotent stem cells using non-synthetic mRNA

L. Rohani [a,b], C. Fabian [a,b], H. Holland [b], Y. Naaldijk [a,b], R. Dressel [d], H. Löffler-Wirth [c], H. Binder [c], A. Arnold [a], A. Stolzing [a,b,e,*]

[a] Fraunhofer Institute for Cell Therapy and Immunology, Leipzig, Germany
[b] Translational Centre for Regenerative Medicine (TRM), University Leipzig, Germany
[c] Interdisciplinary Centre for Bioinformatics (IZBI), Leipzig University, Leipzig, Germany
[d] Institute of Cellular and Molecular Immunology, University Medical Center Göttingen, Göttingen, Germany
[e] Loughborough University, Wolfson School of Mechanical and Manufacturing Engineering, Centre for Biological Engineering, Loughborough, United Kingdom

ARTICLE INFO

ABSTRACT

Here we describe some of the crucial steps to generate induced pluripotent stem cells (iPSCs) using mRNA transfection. Our approach uses a *V. virus*-derived capping enzyme instead of a cap-analog, ensuring 100% proper cap orientation for in vitro transcribed mRNA. *V. virus*' 2′-O-Methyltransferase enzyme creates a cap1 structure found in higher eukaryotes and has higher translation efficiency compared to other methods. Use of the polymeric transfection reagent polyethylenimine proved superior to other transfection methods.

The mRNA created via this method did not trigger an intracellular immune response via human IFN-gamma (hIFN-γ) or alpha (hIFN-α) release, thus circumventing the use of suppressors. Resulting mRNA and protein were expressed at high levels for over 48 h, thus obviating daily transfections. Using this method, we demonstrated swift activation of pluripotency associated genes in human fibroblasts. Low oxygen conditions further facilitated colony formation. Differentiation into different germ layers was confirmed via teratoma assay.

Reprogramming with non-synthetic mRNA holds great promise for safe generation of iPSCs of human origin. Using the protocols described herein we hope to make this method more accessible to other groups as a fast, inexpensive, and non-viral reprogramming approach.

© 2016 The Authors. Published by Elsevier B.V. This is an open access article under the CC BY-NC-ND license (http://creativecommons.org/licenses/by-nc-nd/4.0/).

1. Introduction

The initial approach for deriving iPSCs used retroviral vectors to deliver reprogramming factors into cells (Takahashi & Yamanaka, 2006; Takahashi et al., 2007). Although this method is straightforward, reliable, and easily adoptable by labs, its therapeutic application is precluded because of the risks associated with genomic integration of viral sequences.

Different non-integrating methods for generating human iPSCs have been reported (Stadtfeld et al., 2008; Yu et al., 2009; Jia et al., 2010; Yusa et al., 2009; Warren et al., 2010; Hou et al., 2013). The strengths and weaknesses of these methodologies are under consideration (Robinton & Daley, 2012; Zhou & Zeng, 2013).

Several groups have used mRNA for reprogramming with various degrees of success (Plews et al., 2010; Warren et al., 2012; Yakubov et al., 2010; Tavernier et al., 2012; Mandal & Rossi, 2013; Heng et al., 2013). This method is not well established. An obstacle has been the activation of an innate immune response following mRNA transfection resulting in severe cytotoxicity (Angel & Yanik, 2010; Drews et al., 2012). The mechanism may depend on the nature of the mRNA used for reprogramming (Karikó et al., 2005; Karikó & Weissman, 2007; Karikó et al., 2008). Previous studies incorporated modified nucleosides into mRNA (substitution of cytidine and uridine with pseudouridine and 5-methylcytidine) to abrogate the innate immune response. However residual upregulation of some interferon gene targets has still been detected (Warren et al., 2010; Warren et al., 2012; Mandal & Rossi, 2013).

We recently reported that iPSCs can be generated using non-modified mRNA (Arnold et al., 2012). In this report we will focus on the crucial steps for successfully applying this method.

2. Material and methods

2.1. Cell culture

Human foreskin fibroblast (HFF) was obtained with informed consent (approved by University of Leipzig; Reference No.: 054-09/09,032,009). Human IMR90 fetal fibroblasts were from ATCC Global Bioresource Centre. Fibroblast culture medium was DMEM high glucose

* Corresponding author at: Loughborough University, United Kingdom.
E-mail address: Stolzing@gmail.com (A. Stolzing).

(Gibco) supplemented with 10% FBS (Hyclone). Mouse embryonic fibroblasts (MEFs) were established from dissociated CD1 mouse embryos (13.5–14 d gestation) and inactivated by gamma irradiation (25 Gy).

iPSCs were expanded mechanically and cultured at 5% O_2. iPS medium contained Knockout™ DMEM (Life Technologies) supplemented with 20% Knockout™ serum replacement (KSR) (Life Technologies), 10 ng/ml FGF-basic (Peprotech), 1% nonessential amino acids (Life Technologies), 2 mM L-Glutamine (Life Technologies), 1% penicillin–streptomycin (Life Technologies) and 0.1 mM 2-mercaptoethanol (Sigma-Aldrich). Differentiated parts of the colonies were removed and undifferentiated parts were cut into small pieces. Pieces were lifted up with a filter tip and transferred onto a new plate with pre-coated irradiated MEFs (iMEFs). Passaging was done in the presence of 10 μM rho-associated kinase (ROCK) inhibitor Y-27632 (Calbiochem). Medium was changed at day 2 after cell seeding and then every day until the cells were ready for the next passage. The viral-iPSCs were passaged every 4 days, while the mRNA-iPSCs were expanded once a week.

2.2. Generation of DNA templates

Plasmids based upon the pcDNA3™ (Life Technologies) backbone containing either hNanog, hOct4, hKlf4, hSox2, hc-Myc, hTERT or tagGFP. Cloning strategy and plasmid construction is shown exemplary for hTERT in Supplementary Fig. 1. For in vitro transcription (IVT) up to 2000 nucleotides (nt) either linearized plasmid or PCR product was used as a template. For IVT of mRNA longer than 2000 nt only PCR products were used. All PCR products contained the T7-promoter followed by the gene coding region. Plasmids were linearized at the end of the gene coding region using the appropriate restriction endonuclease (Thermo Fisher or New England Biolabs). Linearized plasmids and PCR products were purified with GeneJet PCR purification kit (Thermo Fisher).

2.3. PCR protocol for IVT templates up to 2000 bp

PCR reactions (25 μl) contained: 1-5 ng plasmid, 2 units Platinum Taq polymerase (Life Technologies), 1× PCR buffer w/o $MgCl_2$, 2.8 mM $MgCl_2$, 0.5 μM of each sense and antisense primer (primer sequences are included in the Supplementary Table 1) and 200 μm of each dNTP (Thermo Fisher). PCR was performed using the TProfessional (Biometra) with the following cycling conditions: 95 °C for 3 min, 35 cycles at 95 °C for 30 s, 60 °C for 30 s, 72 °C for 60 s per 1 kb and a final elongation step 72 °C for 3 min.

2.4. PCR protocol for IVT templates over 2000 bp

PCR reactions (50 μl) contained: 10 ng plasmid, 5 units LongAmp Taq DNA (New England Biolabs), 1× LongAmp Taq Reaction Buffer, 300 μm of each dNTP (Thermo Fisher), 2 μM of each sense and antisense primer (primer sequences are included in the Supplementary Table 1). PCR was performed using the TProfessional (Biometra) with the following cycling conditions: 95 °C for 3 min, 35 cycles at 94 °C for 10 s, 60 °C for s, 65 °C for 50 s per 1 kb and a final elongation step 65 °C for 3 min.

2.5. mRNA IVT

1 μg linearized plasmid or 0.5 μg PCR product was used as template for IVT using the T7mScript Standard mRNA Production System (Epicentre Biotechnologies). The reaction time for the T7-RNA-polymerase transcription step was 3 h for all templates. For hTERT different temperatures were used: 32 °C, 37 °C and 42 °C. Subsequently a cap1 structure was enzymatically added to the IVT-RNA using V. virus-derived capping enzyme and 2′-O-methyltransferase, followed by addition of a Poly(A)tail using mScript™ poly(A) polymerase enzyme according to the manufacture's recommendations (Epicentre Biotechnologies). RNA purification was performed using the GeneJet RNA

purification kit (Thermo Fisher) and a concentration was measured using a NanoDrop1000 photometer (Peqlab). The quality and size of the IVT mRNA was assessed by electrophoresis in a 1% agarose gel stained with ethidium bromide or by capillary electrophoresis with the Agilent 2100 Bioanalyzer (Agilent Technology). For the agarose electrophoresis the RNA samples were loaded with 2× RNA loading dye (Thermo Fisher) directly or after a heat denaturation for 10 min at 70 °C followed by incubation on ice for 3 min. For the capillary electrophoresis the Agilent RNA 6000 Nano kit was used according to the manufacture's protocol.

2.6. mRNA transfection

Transfections were carried out with nucleofection (NHDF–VPD-1001, Lonza), FuGENE HD (Roche), jetPEI (Polyplus) and Lipofectamine 2000 (Life Technologies). Transfections with Nucleofectin and FuGENE HD were carried out as described previously (Arnold et al., 2012).

For jetPEI transfections, the cells (HFF at passages 7–10, and IMR90 fibroblasts at passage 6) were seeded on 6-well-plates (200,000 cells/well) 1 day prior to the experiment. Culture media was changed to OPTI-MEM basal media (Life Technologies) before transfection. Either 3 μg of mRNA for Oct4 (O), Sox2 (S), Klf4 (K), c-Myc (M), Nanog (N), hTERT (T) and GFP or 3 μg mixture of the reprogramming factors-mRNA (equal amounts of each factor) was diluted in 150 mM sodium chloride solution (PolyPlus). JetPEI was dispersed in 150 mM sodium chloride solution. These components were incubated 30 min at RT before being dispensed to culture media. 4 h after transfection the medium was changed to either fibroblast or iPS medium.

For Lipofectamine 2000 transfections, HFFs were seeded on 6-well-plates (200,000 cells/well) at passage 3 1 day prior to experiments. 3 μg of mRNA and Lipofectamine 2000 were diluted in OPTI-MEM basal media and then delivered to culture media after 20 min incubation at RT. 4 h after transfection the medium was changed to fibroblast medium.

2.7. Toxicity assay

Cells were seeded on 48-well plates at a density of 20,000 cells per well. One day after seeding, the cells were incubated with mRNA-jetPEI and mRNA-lipofectamine 2000. Viability was detected using the MTT assay, 24 h, 48 h and 72 h after transfection. Briefly, the medium of the cells was replaced with 250 μl of fresh fibroblast medium and 25 μl of MTT solution (Thiazylblau in 1× PBS⁻, Applichem) for each well, followed by 4 h incubation at 37 °C. MTT solution was aspirated after 4 h and reaction stopped by an addition of 250 μl of stop solution containing 50% dimethyl sulfoxide (VWR International) and 50% SDS solution (Merk Millipore). Plates were incubated at 37 °C for 1 h and the absorbance was measured using a microplate reader (Tecan Infinity Pro 200 series) at 550 nm and 630 nm as a reference wavelength.

2.8. Measurement of interferons by ELISA

Level of hIFN-γ and -α was detected in the supernatant of mRNA-transfected cells after the first transfection by ELISA (Mini ELISA Development Kit, Peprotech) according to the manufacturer's instructions.

2.9. Flow cytometry

mRNA-transfected cells were trypsinized 24 h, 48 h and 72 h after transfection, washed with PBS⁻ and fixed in 4% paraformaldehyde (Thermo Scientific) for 15 min. Fixed cells were washed with PBS⁻/1% BSA, then permeabilized with 0.2% Tween 20 (Sigma) in PBS⁻ at 37 °C for 10 min. Cells were blocked with PBS⁻ containing 10% BSA (Sigma) at 37 °C for 30 min, then incubated for 1 h at 4 °C with the following primary antibodies: Oct4 (1:600, Cell Signaling), Sox2 (1:300, Cell Signaling), c-Myc (1:200, Cell Signaling), Nanog (1:400, Cell Signaling), Klf4

(1 μg, Thermo Scientific), and hTERT (1:50, Thermo Scientific). Cells were incubated with secondary antibodies Alexa fluor 488 (1:2000, Invitrogen) and Alexa fluor 546 (1:2000, Invitrogen) for 1 h at 4 °C, suspended in PBS$^-$ and analyzed by flow cytometry (BD FACS Calibur). Non-transfected cells and cells stained with secondary antibody were used as controls. All other data were compared to the controls. Ten thousand gated events were collected per sample.

2.10. Reprogramming

Human foreskin or IMR90 fibroblasts were seeded on 6-well-plates pre-coated with 0.1% gelatin (Sigma-Aldrich). Cells were transferred to 5% O_2 1 day prior to the experiment. Repeated mRNA transfections were performed using a jetPEI transfection. Different factor combinations, ONT, OSK and OSKMNT were tested. 4 h after transfection the medium was changed to iPS medium equilibrated at 5% O_2 for approximately 2 h before use. Transfections were performed every 48 h for 2 weeks. mRNA-iPS colonies were manually picked and transferred on iMEFs.

2.11. Immunostaining

mRNA-transfected cells were fixed with 4% paraformaldehyde 24 h after transfection, washed and permeabilized with 0.5% Triton X-100 in PBS$^-$ (Life Technologies) for 30 min and blocked with 10% FCS in PBS$^-$ for 1 h. Cells were incubated with primary antibodies in PBS$^-$, 1% FCS, and 0.5% Triton X-100 at 4 °C for 1 h. After washing 3 times, cells were incubated with secondary antibody in PBS$^-$ for 30 min at 4 °C. The primary antibodies were Oct4 (1:400), Sox2 (1:400), c-Myc (1:800), and Nanog (1:400) (all from Cell Signaling Technology). Secondary antibody was Alexa flour 488 (1:1000, Invitrogen). Nuclei were counterstained with 4, 6-diamidino-2-phenylindole dilactate (DAPI; 1:10,000, Sigma). HFF-mRNA-iPS colonies and HFFs were fixed and stained using the above procedure. All cells were visualized using a fluorescence microscope (Axio Observer, Zeiss).

2.12. Teratoma formation

The teratoma formation assay was performed as previously described (Dressel et al., 2009; Dressel et al., 2010). The experiments have been approved by the Niedersächsisches Landesamt für Verbraucherschutz und Lebensmittelsicherheit. Immunodeficient RAG2$^{-/-}$ γc$^{-/-}$ mice were injected subcutaneously with 1×10^6 IMR90-mRNA-iPSCs in 50 μl PBS$^-$ mixed with 50 μl Matrigel (BD Biosciences). Tumor growth was monitored weekly by palpation and size was recorded using linear calipers. Animals were sacrificed when a tumor diameter of 1 cm was reached or after 3 months. Autopsies were performed and tumor tissue was placed in phosphate-buffered 4% formalin for 16 h and then embedded in paraffin. For histological examination, tissue sections (2 μm) were stained with hematoxylin and eosin.

2.13. Karyotyping

IMR90-mRNA-iPSCs and IMR90 fibroblasts were incubated with 0.1 ml Colcemid (100 mg/l isotonic NaCl solution) (Life Technologies) for 3 h at 37 °C. Cells were collected by cell scraper and placed in a hypotonic solution (0.075 M KCl solution) (B. Braun Medical Inc.) at RT. Cells were centrifugation and fixed with methanol (VWR) and acetic acid (VWR) (3:1) for 5 min followed by spreading the cells on microscopic glass slides and let air dry. Trypsin-Giemsa (Dr. K. Hollborn & Söhne GmbH & Co. in Leipzig) staining (GTG-banding) of the chromosomes was performed by treating the glass slides with trypsin solution (0.5 g trypsin in 250 ml isotonic NaCl solution) for 10-20s, washed twice with 0.9% NaCl and stained using Giemsa solution (5 ml Giemsa stock solution in 150 ml Soerensen buffer) for 5 min. The total analyzed metaphases for IMR90 fibroblasts were 25 and for IMR90-mRNA-iPSCs

were 20. Analysis of karyotyped cells was performed using GeneASI BandView software (Applied Spectral Imaging).

2.14. Quantitative RT–PCR

Total RNA was extracted using Trifast reagent according to the manufacturer's instructions (Peqlab) and treated with DNaseI (Thermo Scientific). cDNA was synthesized using Superscript III (Life Technologies) and Oligo(dT)$_{18}$-Primers (Thermo Scientific) at 50 °C for 1 h. cDNA was used as PCR template in a 1:10 dilution and each sample was run in triplicate. Quantitative PCR was done using Express SYBR Green ER qPCR Supermix Universal (Life technologies), additional 1× SybrGreen I (Life technologies) and 0.2 μM primer (Supplementary Table 2) each on the DNA engine Opticon2 (Biorad) with the following cycle conditions: primary denaturation at 95 °C for 3 min, 35 cycles with 30 s at 95 °C, 30s at 60 °C (36B4, Sox2)/55 °C (Oct4, Nanog, Klf4, c-Myc) and 30 s at 72 °C followed by fluorescence measurement. Absolute quantification was done for every single gene by dilution series of plasmid positive controls and set in relation to the reference gene 36B4.

2.15. Gene expression profiling

Six different samples including HFFs, HFF-mRNA-iPSCs, IMR90 fibroblasts, IMR90-mRNA-iPSCs, foreskin-derived-viral-iPSCs (HFF-viral-iPS) and hESCs control (H9 cell line) were used. At least 30 iPS colonies were used per iPS sample. Total RNA was extracted with TriFast and purified using GeneJet RNA purification kit (Thermo scientific) according to protocol. RNA integrity was confirmed using Agilent 2100 bioanalyzer (Agilent technologies). Total RNA was depleted of ribosomal RNA using the "RiboMinus Kit" (Life technologies) followed by first and second cDNA synthesis as well as intermediate in vitro transcription using the "WT cDNA Synthesis and Amplification Kit" according to the manufacturer's instructions (Affymetrix). cDNA was fragmented and labeled with the "WT Terminal Labeling Kit" (Affymetrix) and hybridized to Human Genome 1.0 ST Arrays. Washing and staining steps were performed with the Affymetrix Fluidics Station FS400. Arrays were scanned with a third-generation Affymetrix "GeneChipScanner 3000" equipped with the "7G" upgrade.

2.16. SOM portraying of overall expression landscapes

A Self-Organizing Map (SOM) was trained and analyzed as described previously (Wirth et al., 2011; Wirth et al., 2012). The total gene expression matrix of (N = 6 samples) × (M = 32,321 genes) was transformed into a reduced matrix where the genes were clustered into K = 900 microclusters called metagenes after appropriate normalization and centralization of the input expression data (Wirth et al., 2011). SOM-machine learning provided strong visualization capabilities: the expression values of the metagenes in each of the samples were transferred into a two-dimensional 30 × 30 mosaic picture 'portraying' the expression landscape of each sample using an appropriate color gradient: red reflects strong over-expression compared to the mean expression of a metagene; yellow and green tones indicate intermediate levels with low or no differential expression; and blue corresponds to under-expression. Each metagene collected similar 'profiles' of single genes in the samples measured. Moreover, similar metagene profiles were usually arranged in neighboring pixels in the maps thus forming extended over- and under-expression spots. Importantly, each gene was associated with one and the same metagene and thus with the same position in all individual sample images.

2.17. Statistical analysis

All experiments were repeated three times. One-way analysis of variance (ANOVA) followed by Tukey test was used to determine whether observed differences were statistically significant between different

experimental conditions. P < 0.05 was considered statistically significant using Sigma plot. Data were presented as mean ± SEM.

3. Results

3.1. Producing mRNA

For most factors (Oct4, Nanog, Klf4, Sox2) using linearized plasmid or PCR products as IVT template lead to a high yield of full-sized IVT-RNA (Fig. 1B). The IVT template consisted of the open reading frame (ORF) of the gene of interest with a 5′Kozak translation initiation signal and a T7 promoter sequence (Fig. 1A). The PCR products consisted of an extended T7 promoter sequence (−27 to +1) to increase the promoter strength (Tang et al., 2005). For c-Myc and TERT a PCR-derived template was superior to linearized plasmid which otherwise gave no (TERT) or minimal (c-Myc) yield. c-Myc's ORF is a difficult IVT template due to >80% G/C content. However reduction of the template size to the essential elements allowed for efficient transcription. All factors had ORFs below 1.5 kb except for the ORF of TERT which was over 3 kb.

While the IVT produced full length TERT-RNA, there were also smaller RNA fragments produced. This could be attributed to either a sequence inside the ORF resembling a T7 RNA polymerase termination signal or to secondary structures that may be problematic for the T7-RNA-polymerase to resolve. Hence, we tested a lower reaction temperature for the IVT to enable the T7-RNA-polymerase to override a potential termination signal and a higher reaction temperature to denature possible secondary structures. While the lower temperature yielded

the same IVT RNA products mixture of small and full-length IVT-RNA, the higher temperature leads to the full-length IVT RNA product without smaller fragments. This suggests that secondary structures were interfering with IVT (Supplementary Fig. 2). IVT-mRNA showed high quality before and after PolyA-tailing (Fig. 1C) and were stable for 18 months at −80 °C (Fig. 1C).

3.2. Transfection efficiency

The efficiency of various mRNA transfection systems (electroporation, FUGEN HD, Lipofectamine 2000 and jetPEI) were compared using of GFP mRNA transfection. jetPEI and Lipofectamine 2000 showed a significantly better transfection rate (Supplementary Fig. 3).

3.3. Cytotoxicity of transfection reagents

JetPEI and lipofectamine 2000 were compared for effect on cell viability in combination with each mRNA factor introduced. Comparison revealed no significant differences in the viability of the transfected cells up to 72 h post-transfection (Fig. 2A). Cells transfected with jetPEI reagent showed a trend to be more viable than Lipofectamine 2000. Consequently, jetPEI was used in all following experiments.
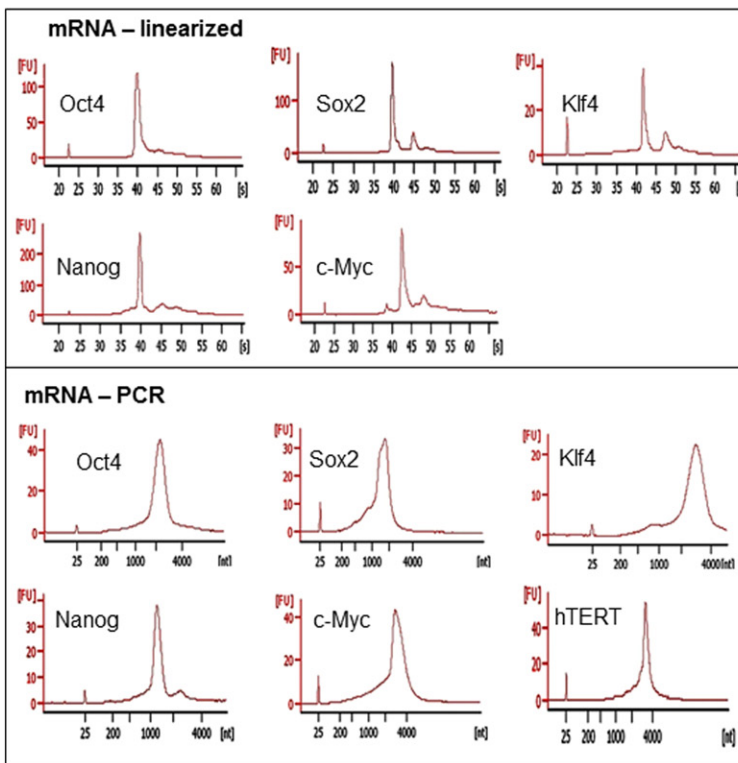
3.4. Immune response

To identify a cellular immune response following mRNA transfection, levels of hIFN-γ and -α emitted by the transfected cells were
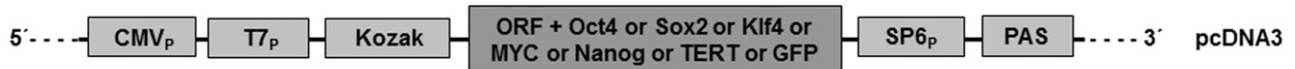
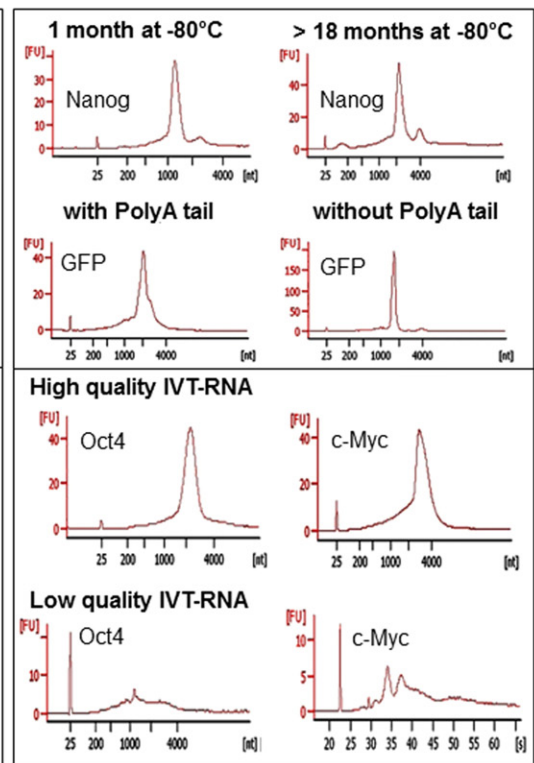Fig. 1. Quality control of IVT-RNA. A) A representation of the reprogramming constructs (containing Oct4, Sox2, Klf4, c-Myc, Nanog, TERT or GFP) in pcDNA3. IVT-RNA samples were analyzed using Agilent Bioanalyzer. B) Comparison of IVT-RNA using either linearized plasmid or PCR products as IVT template. C) Quality control of fresh IVT-RNA and stored IVT-RNA (at −80 °C), IVT-RNA with and without PolyA-tail and examples for high and low quality IVT-RNA.
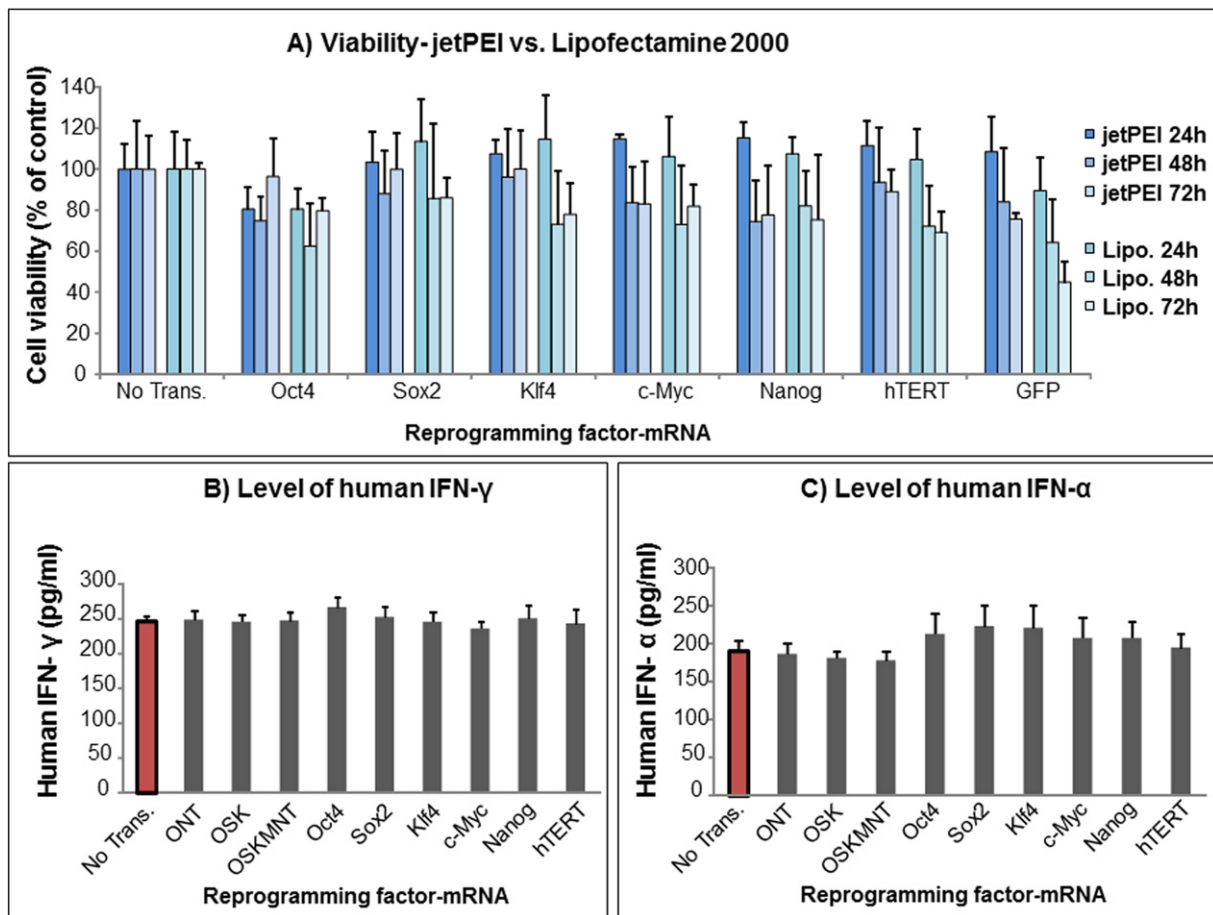
Fig. 2. Stress of reprogramming factors-encoding mRNA. A) Comparison of viability after transfection. Data were presented as percentage of cell viability compared to non-transfected cells which set as a value = 100. Cells used for analysis were foreskin fibroblasts derived from 3 different donors at passage 3. B) & C) The level of hIFN-γ and -α in the supernatant of transfected cells following mRNA transfection. Cells used for analysis were foreskin fibroblasts derived from 3 different donors at passage 3. Graphs represent means ± SEM; n = 3. Lipo. = Lipofectamine 2000. No trans. = Non-transfected cells. ONT = Oct4, Nanog, hTERT. OSK = Oct4, Sox2, Klf4. OSKMNT = Oct4, Sox2, Klf4, c-Myc, Nanog, hTERT.

measured by ELISA. Compared to non-transfected cells, no significant differences in levels were observed in the supernatant of transfected cells using various factor combinations or single factors (Fig. 2B & C).

3.5. mRNA-transfection

To generate mRNA-iPSCs, fibroblasts were transfected with different mRNA-factor combinations. Results have been summarized in Supplementary Fig. 5 and Supplementary Table 3. Formation of cellular aggregates from mesenchymal to epithelial (MET) transition was observed in five donor cells (foreskin 1, foreskin 1–1, foreskin 2, foreskin 3, and IMR90 fibro.) and they formed cellular aggregates after 2–4 transfections (Supplementary Fig. 5 and Supplementary Table 3). For some of the donors (foreskin 2 & 3) only small cell aggregates were formed which grew very slowly and could not be passaged more than once on iMEFs. The colonies from foreskin fibroblasts (foreskin 1) and IMR90 fibroblasts showed the highest stability and could be passaged on iMEFs (5 passages for foreskin 1 & over 37 passages for IMR90), thus they were used for generation of stable cell lines and different pluripotency characterization tests.

3.6. Protein expression of reprogramming factors

Persistence of reprogramming proteins in transfected cells was monitored using flow cytometry. High expression levels were found for all factors following mRNA transfection (Fig. 3A). It was observed that between 50% (GFP) to over 90% (c-Myc) of the cells expressed the reprogramming proteins (Fig. 3A). Maximal protein expression of

reprogramming factors occurred between 24 h to 48 h after transfection (Fig. 3B). In all instances the percentage of positive cells remained stable between 24 h and 48 h but decreased 72 h after transfection (Fig. 3B).

More than 90% of the fibroblasts were positive for Oct4, Sox2, Klf4, c-Myc and Nanog protein 24 h and 48 h after transfection (Fig. 3B). GFP and TERT were expressed significantly less efficiently compared to the other factors. The percentage of GFP positive cells was significantly (§$P < 0.01$) lower compared to the other factors 72 h after transfection (Fig. 3B). The expression of hTERT-mRNA was significantly (*$P < 0.01$, +$P < 0.01$) lower compared to the other factors at 24 h, 48 h and 72 h after transfection (Fig. 3B). The above results were confirmed using mean fluorescent intensity (MFI) of positive cells. It was found that the protein level for all factors was maximal 24 h and 48 h after transfection and decreased significantly (**$P < 0.01$) 72 h after transfection for Sox2, Klf4, c-Myc and Nanog (Fig. 4B).

To confirm that reprogramming proteins correctly localized as endogenous protein, the mRNA-transfected cells were stained using immunocytochemistry. The results demonstrated that each of the factors was robustly expressed and correctly localized to the nucleus (Fig. 4A). No reprogramming proteins were detected in non-transfected fibroblasts (Supplementary Fig. 4).
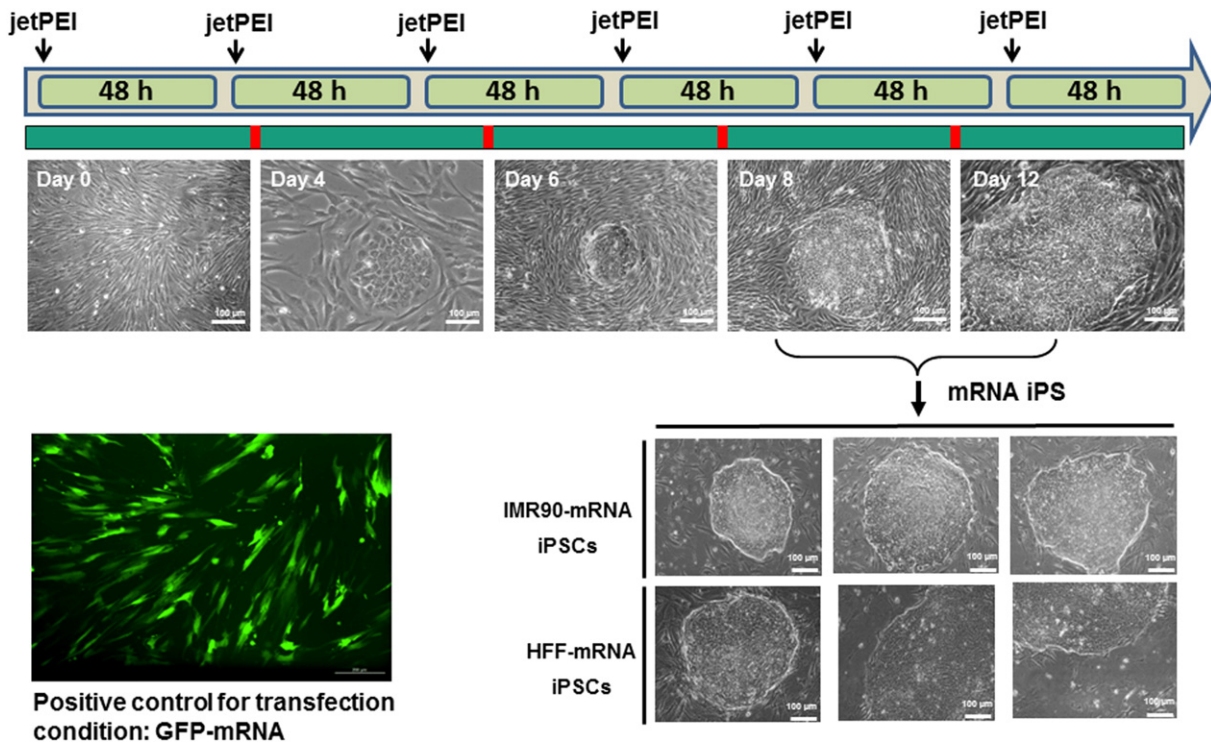
3.7. Reprogramming

For the establishment of stable mRNA-iPSCs, fibroblasts (foreskin & IMR90) were transfected with different factor combinations using jetPEI, every 48 h over a period of 2 weeks. Cells underwent mesenchymal-epithelial transition based upon morphological changes
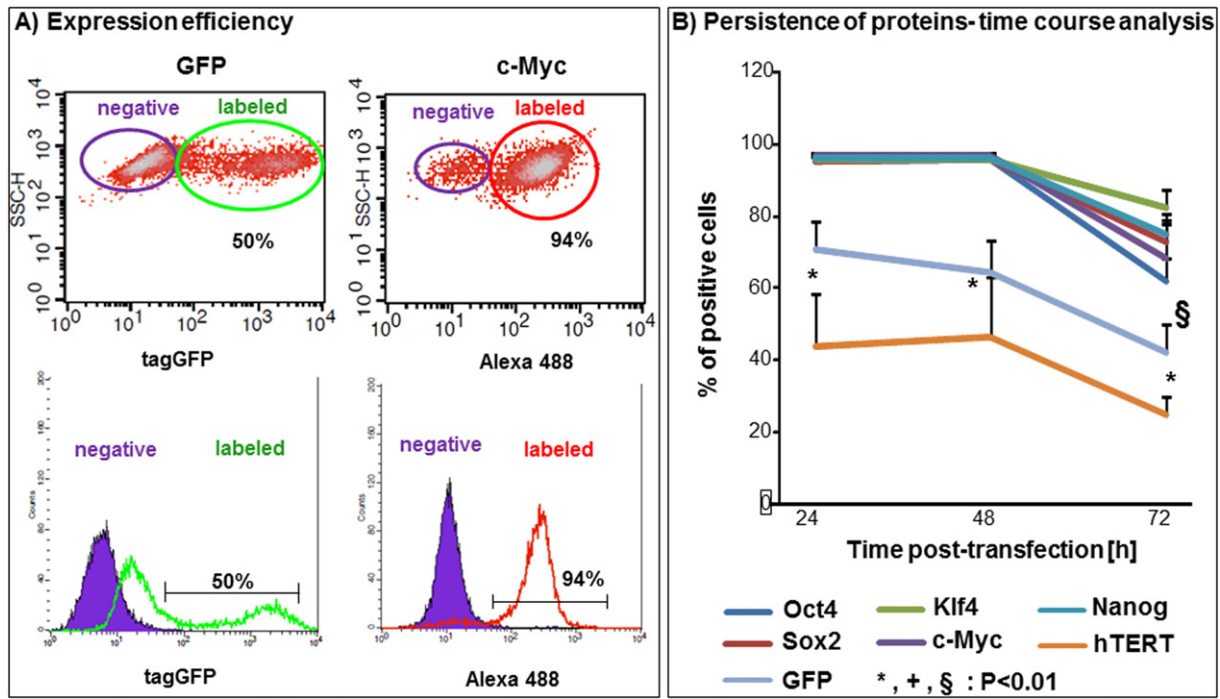
Fig. 3. Protein expression of reprogramming factors. A) The graphs show expression efficiency of reprogramming proteins after a single mRNA transfection. Non-transfected cells and cells stained with secondary antibody were used as controls. B) Persistence of reprogramming proteins in the transfected cells monitored over 72 h using the gating strategy from A. Cells used for analysis were foreskin fibroblasts from 3 different donors at passage 3. Graphs represent means ± SEM. n = 3. *P < 0.01 = The percentage of hTERT positive cells 24 h, 48 h, and 72 h after transfection compare to the other factors (Oct4, Sox2, Klf4, c-Myc and Nanog) at 24 h and 48 h after transfection. +P < 0.01 = The percentage of hTERT positive cells 72 h after transfection compare to the other factors (Sox2, Klf4, c-Myc and Nanog) at 72 h after transfection. §P < 0.01 = The percentage of GFP positive cells 72 h after transfection compare to the other factors (Oct4, Sox2, Klf4, c-Myc and Nanog) at 24 h and 48 h after transfection.
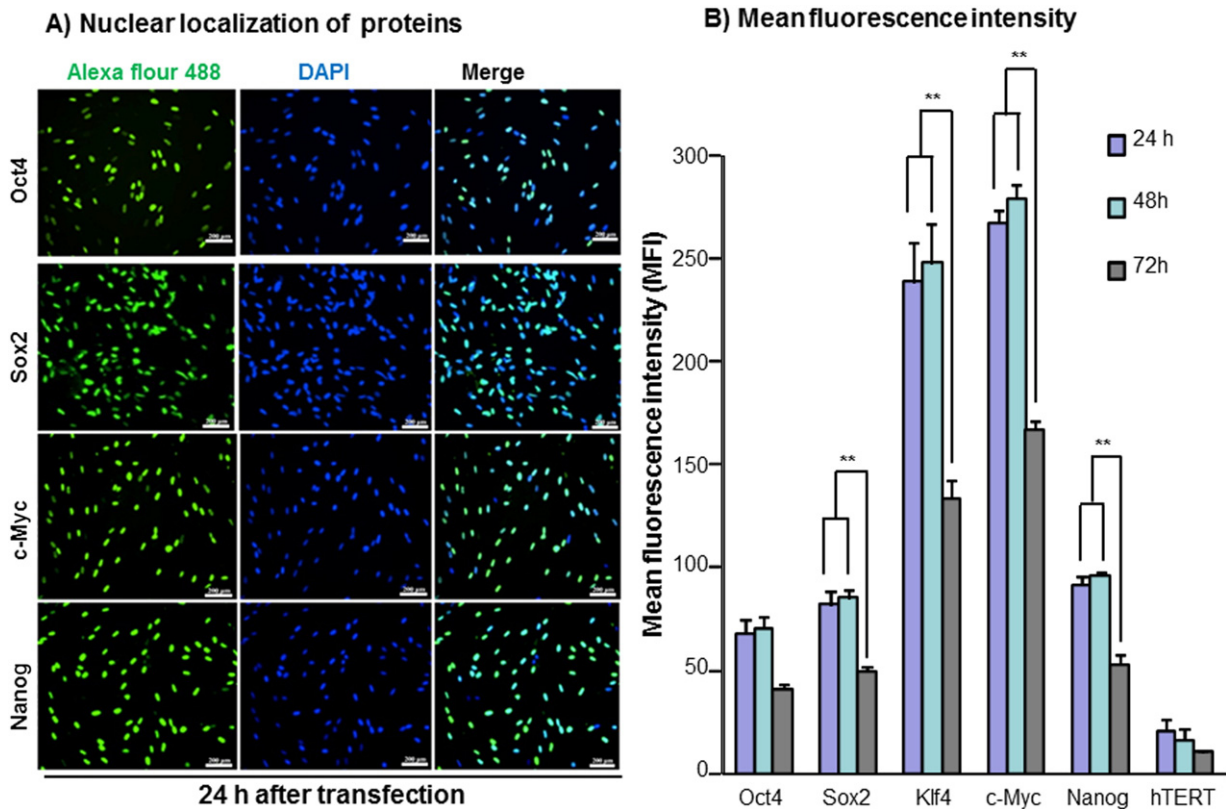
Fig. 4. Nuclear localization and mean fluorescence intensity of reprogramming proteins. A) Proteins of reprogramming factors derived from the transfected mRNAs localized in the nucleus of transfected cells 24 h after transfection. Cells used for immunostaining were foreskin fibroblasts at passage 3. Scale bars represent 100 μm. B) The mean fluorescence intensity of human foreskin fibroblasts derived from 3 different donors represents the protein level for the analyzed reprogramming factors at different time points after single mRNA-transfection. Graphs represent means ± SEM; n = 3; (**P < 0.01).

Fig. 5. Reprogramming of human fibroblasts using mRNA. Morphological changes observed following transfections with jetPEI-mRNA. Transfection was controlled using GFP-mRNA (left-lower picture). Arrows indicate the timing for repeated transfections with jetPEI. Images show human foreskin fibroblasts on day 0, followed by the formation of small clusters with a compact morphology (epitheliod morphology) on day 4 (upper pictures). The first iPS colony-like structure was observed on day 6 and well-defined border colonies appeared at day 8. Mature colonies with prominent nucleoli were visible on day 12 (upper pictures). The right-lower pictures represent HFF- and IMR90-mRNA-iPS colonies expanded on iMEF. HFF = human foreskin fibroblasts. HFF-mRNA-iPSCs = mRNA iPS cells derived from human foreskin fibroblasts. IMR90-mRNA-iPSCs = mRNA iPS cells derived from human IMR90 fibroblasts. Scale bars represent 100 μm.

that were observed during repeated transfections (Fig. 5 & Sup. Fig. 5). Switch of fibroblast morphology to a compact, epithelioid morphology was observed 4 days after the first transfection, followed by the emergence of typical hESC-like colonies with tight morphology by day 6. Well defined borders colonies were appeared at day 8 and mature colonies with prominent nucleoli were visible at day 12 (Fig. 5). Two iPS cell lines could be established (HFF-mRNA-iPSCs & IMR90-mRNA-iPSCs).

3.8. Teratoma assay

Trilineage differentiation potential was confirmed in vivo by the formation of teratomas derived from IMR90-mRNA-iPS colonies. Six mice injected with iPSCs developed tumors within 7 weeks after injection of the cells. Two of them were fully developed teratomas and showed clearly all three germ layers. Control fibroblasts injected were not causing any tumor growth. The results of hematoxylin–eosin staining showed cell types of the three germ layers in the teratoma sections (Fig. 6A).

3.9. Immunostaining

The expression of pluripotency markers in mRNA-iPSCs was assed using immunostaining. The results showed the expression of pluripotency markers in HFF-mRNA-iPS colonies compared to their donor fibroblasts (foreskin). Furthermore, nuclear localization of Oct4 and Nanog was confirmed (Fig. 6B & Sup. Fig. 4B).

3.10. Karyotyping

To determine possible chromosomal aberrations following mRNA reprogramming, GTG-banding was performed. The results of karyotype analyses revealed similar chromosomal aberrations in IMR90-mRNA-

iPSCs as compared to parental IMR90 fibroblasts and no increase in aberrations was observed upon reprogramming (Fig. 6C and Supplementary Table 4).

Parental IMR90 fibroblasts displayed numerical chromosomal aberrations such as hyperdiploidy, hypotriploidy, triploidy, hypertriploidy, hypotetrapoidy, hypertetraploidy and hypohexaploidy. IMR90-mRNA-iPSCs; however, showed a trend to reduce numerical chromosomal aberrations (Supplementary Table 4). Some of the numerical chromosomal aberrations such as hypertriploidy, hypertetraploidy and hypohexaploidy were no longer observed in IMR90-mRNA-iPSCs. Furthermore, IMR90-mRNA-iPSCs demonstrated a trend to decrease total and recurrent structural chromosomal aberrations compared to IMR90 parental fibroblasts (Supplementary Table 4).

3.11. Pluripotency genes

IMR90-mRNA-iPS and HFF-mRNA-iPS colonies were passaged at least 3 times before the expression of pluripotency genes were analyzed by qRT-PCR. Using a non-integrating reprogramming approach with mRNA offers the advantage that mRNA will degrade after the reprogramming procedure and does not interfere with analyzing mRNA-expression levels.

In HFF-mRNA-iPS colonies Nanog, Oct4 and Klf4 were abundantly expressed compared to the HFF donor showing no Nanog and very low expression of Oct4 and Klf4 (Supplementary Fig. 6). In contrast IMR90 fibroblasts already had a high basic expression of Oct4, Sox2 and Klf4. In IMR90-mRNA-iPS colonies the expression of Sox2 and Oct4 increased during reprogramming. Klf4 expression went down at early passages but increased at later passages again. As in HFFs, Nanog expression was induced in the IMR90-mRNA-iPSCs and increased with higher passages (Fig. 7A).
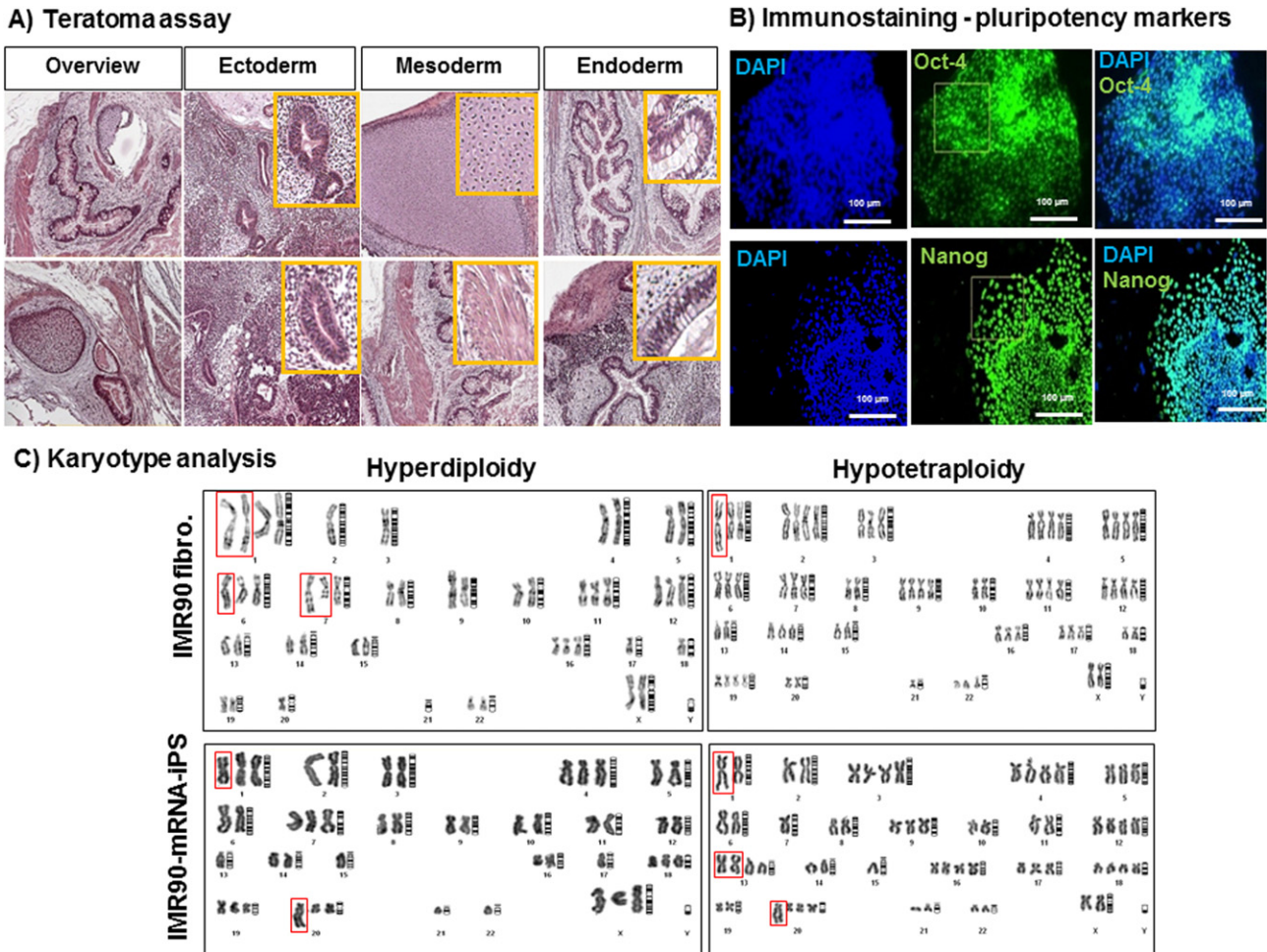
Fig. 6. Characterization of mRNA-iPSCs. A) Teratoma formation assay. The pictures show hematoxylin–eosin staining of teratoma sections derived from IMR90-mRNA-iPS colonies (passage 8) following subcutaneously injection. Cell types of the three germ layers have been shown in the teratoma sections. B) Immunostaining for pluripotency markers. Pictures show the expression of pluripotency markers in HFF-mRNA-iPS colonies at passage 5. Scale bars represent 100 μm. C) Karyotype analyses of mRNA-iPSCs. Chromosomal GTG-banding analysis of IMR90-mRNA-iPSCs (passage 37) and IMR90 parental fibroblasts (passage 14) are shown. The pictures show presence of hyperdipoloidy and hypotetraploidy in both IMR90 fibroblasts and IMR90-mRNA-iPSCs.

3.12. SOM expression portraits

We generated SOM portraits of the expression data to get detailed insights into comprehensive and individual structures of the expression landscapes. Therefore we trained a SOM using microarray expression data of our samples. The method 'portrays' the individual expression landscape of each sample in terms of mosaic images. The portraits generated are similar within the groups reflecting homogeneity of their overall expression landscapes (Fig. 7B). Visual inspection of the patterns in the portraits reveals two dominant characteristics, namely spots of over-expressed metagenes (i.e. red colored pixels) in the bottom-left and top-right regions of the map. The former collects genes up-regulated in the HFF sample, the latter collects genes up-regulated in stem cell controls (right edge) and IMR90 samples (top and right edge). In particular, the portrait of IMR90 fibroblast differs from the HFF fibroblast showing a global expression pattern closer to the stem cell controls. The pattern of IMR90-mRNA-iPS resembles the hESC sample and particularly the HFF-viral-iPS control (see the red spot in the top right corner of the map, collecting up-regulated genes in the respective samples). The molecular phenotypes of IMR90-mRNA-iPS, the viral iPS and the hESC sample are thus very similar as seen by the overall expression landscape portraits.

4. Discussion

In this section, we briefly take up some points requiring further discussion regarding the results of the iPSCs analysis and then consider the steps that are of particular technical interests with this method of non-synthetic mRNA reprogramming.

### 4.1. Teratoma assay and pluripotency markers

mRNA-iPSCs showed hESC-typical pluripotency markers, morphology, and differentiation into all three germ layers. The formation of teratomas shows the feasibility of non-modified mRNA for generation of fully reprogrammed iPSCs. This finding is in contrast with some studies showing only the activation of pluripotency-associated genes upon delivery of non-modified mRNAs. Using non-modified RNA, Plew et al. did not attain complete reprogramming to fully characterized iPSCs, since they just obtained small cell aggregates which failed to expand on to MEFs (Plews et al., 2010). Yakubov et al. obtained alkaline phosphatase positive colonies after non-modified mRNA transfection, however; no differentiation analysis and no teratoma formation were done, and thus it is difficult to evaluate the pluripotency of their iPSCs (Yakubov et al., 2010). Other studies have shown teratoma formation of iPSC colonies generated by only modified RNA and not non-modified RNA
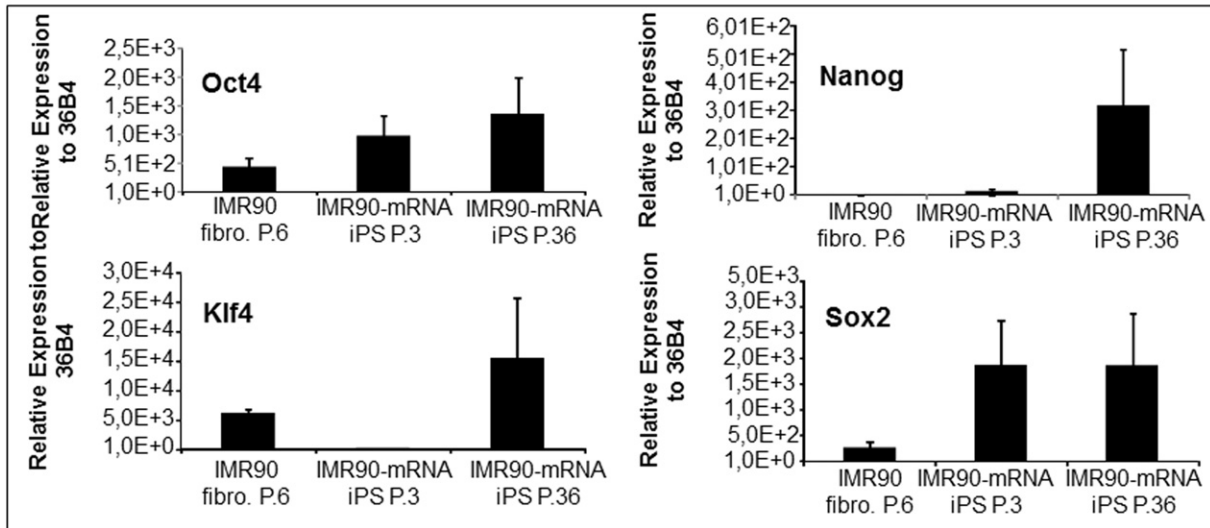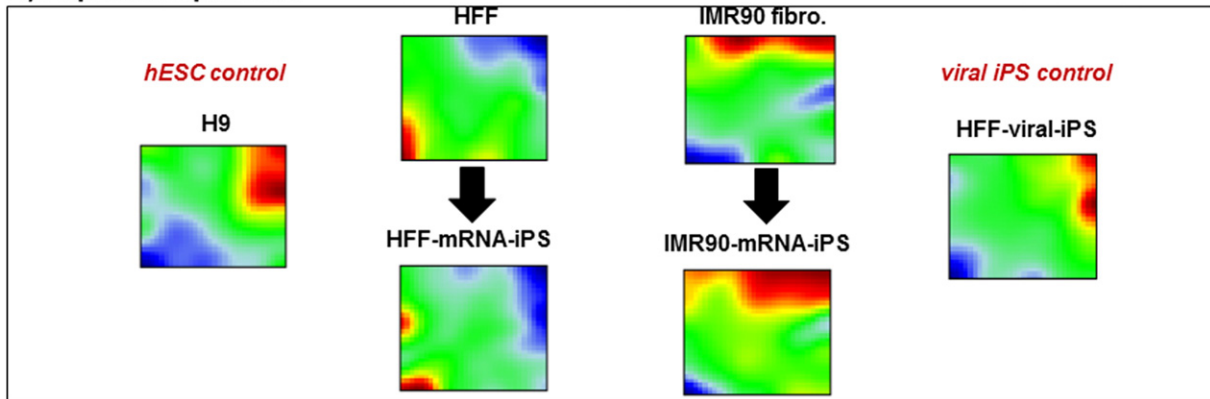
Fig. 7-. Molecular characterization of mRNA-iPSCs. A) Expression of pluripotency-related genes in IMR90-mRNA-iPS colonies (passage 3 & passage 36) and IMR90 parental fibroblasts (passage 6) analyzed by qRT-PCR. 36B4 was used as housekeeping gene. P.3 = passage 3. P.36 = passage 36. B) SOM portraying of the microarray expression resulted from 6 different samples. The samples used contain 1) HFF (passage 7), 2) HFF-mRNA-iPSCs (passage 3), 3) IMR90 fibroblasts (passage 6), 4) IMR90-mRNA-iPSCs (passage 11), 5) foreskin-derived-viral-iPSCs (HFF-viral-iPS) (passage 20), 6) and hESCs control (H9 cell line).

(Warren et al., 2010; Heng et al., 2013). Therefore, this is the first report of teratoma formation from the mRNA-iPSCs generated by non-modified RNA.

4.2. Karyotype

There is currently conflicting data regarding chromosomal abnormalities of iPSCs. Some publications suggest that chromosomal aberrations occur upon reprogramming followed by further expansion of the reprogrammed cells (Hussein et al., 2011; Gore et al., 2011; Lister et al., 2011; Mayshar et al., 2010). Heng et al. demonstrated that chromosomal changes can occur during adaptation of the iPSCs to prolonged culture conditions (Heng et al., 2013). They reported chromosomal abnormalities in 4 out of 7 stable iPS cell lines following prolong passaging (Heng et al., 2013). In another study karyotype analysis on more than 1700 human iPS cell lines were performed and the occurrence of chromosomal aberrations was 12.5% (Taapken et al., 2011). Two reports noticed that reprogramming could restore chromosomal aberrations in iPSCs generated from disease-associated chromosomal abnormality (known as a ring chromosome) (Bershteyn et al., 2014; Kim et al., 2014). In this study, IMR90-mRNA-iPSCs maintained some of the pre-existing chromosomal aberrations of the parental IMR90 fibroblasts and no structural and numerical aberrations were acquired upon reprogramming. mRNA-iPSCs displayed a tendency for more stability

and reduction of chromosomal aberrations. Numerical chromosomal aberrations such as hypertriploidy, hypertetraploidy and hypohexaploidy were not observed in mRNA-iPSCs which might indicate a selective advantage favoring normal karyotypes upon iPS generation or confirm that reprogramming itself revert chromosomal aberrations to a more stable karyotype.

4.3. Pluripotency associated gene expression

HFF- as well as IMR90-mRNA-iPSCs could be characterized by their pluripotency gene expression. The induced expression of Nanog in particular is essential for the pluripotency transcriptional circuitry and mediating self-renewal maintenance of stem cells (Silva et al., 2009; Theunissen et al., 2011).

IMR90 cells are of fetal origin which may explain the pre-existing expression of several pluripotency genes. The expression of Klf4 in fetal lungs is induced by oxygen (Shields et al., 1996; Jean et al., 2013). Hence, the intermittent down-regulation of Klf4 at passage 3 of the IMR90-mRNA-iPSCs may be due to cultivation in hypoxia with a subsequent up regulation attributable to the general pluripotency profile of the proliferating IMR90-mRNA-iPSCs.

The SOM analysis of the gene expression showed that the portrait of IMR90-mRNA-iPSCs features a molecular phenotype closely resembling

hESC and viral-iPSCs while the HFF-mRNA-iPSCs are more comparable to the original HFF.

HFF and IMR90 fibroblast already differ in their basic gene expression. The fetal IMR90 fibroblast reveals a portrait that resembles more the portrait of the hESC than the adult HFF.

In general, fetal and adult fibroblasts have different properties. Navarro et al. showed different gene expression pattern between fetal and adult lung fibroblast especially regarding components of the TGF-β family signaling pathways (Navarro et al., 2009). Since these pathways are involved during embryonic development and later on regulate proliferation, tissue repair and differentiation, it seems likely that they are also involved in the success of reprogramming.

4.4. Technical advances

The mRNA-based reprogramming has not yet been used routinely in many laboratories. In this paper we describe some crucial steps for the efficient generation of mRNA-derived iPSCs, focusing on some crucial technical details for the successful application of this method.

4.5. Non-synthetic mRNA

Our protocol allows for the efficient IVT production of 5′-capped and 3′-polyadenylated mRNA with easy modifications even for difficult templates with a high G/C content or a long sequence. The use of PCR products as IVT template removes the need to clone IVT expression cassettes if the ORF of the gene is already available. The alternative system for mRNA production eliminates the need to remove residual 5′-triphosphates from non-capped IVT-RNA which is necessary step for cap analogs. The cap analog system produces only ~80% capped RNA. Instead, our approach is to use a *V. virus*-derived capping enzyme which ensures 100% capped IVT-RNA transcripts. The additional use of the *V. virus*-derived 2′-O-Methyltransferase creates a cap1 structure found in higher eukaryotes and providing a higher translation efficiency (Kuge et al., 1998).

4.6. Reduced immunogenicity and cytotoxicity following mRNA transfection

It has been discussed that transfection-associated activation of innate intracellular immunity pathways triggered by foreign nucleic acid like IVT-RNA leads apoptosis (Warren et al., 2012; Angel & Yanik, 2010; Drews et al., 2012). This is one of the main barriers for successful induction of pluripotency through mRNA-reprogramming (Drews et al., 2012). Exogenous RNAs and particularly the uncapped 5′-triphosphate (3pRNA) end-RNAs are pathogen-associated molecular pattern for toll-like receptors and RNA sensors (RIG-I and PKR) (Angel & Yanik, 2010; Karikó et al., 2005). Consequently, a key step in cellular mRNA processing is the addition of a 5′ cap structure. Different capping systems could be inserted to the 5′-end of RNA. To suppress the immune response following mRNA transfection, Warren et al. utilized cap analog ARCA with modified nucleosides. Even so upregulation of a number of interferon response genes was observed (Warren et al., 2010). Consequently, they applied recombinant B-18-R-protein, as a suppressor of type I interferon to inhibit innate immune response. Application of interferon suppressors such as B-18-R-protein might have an effect on reprogramming. Mah et al. claimed that B-18-R supplementation yielded Nanog-positive iPSCs (Mah et al., 2011). Some groups have recently clarified the role of B-18-R-protein on reprogramming (Yoshioka et al., 2013). The use of B-18-R-protein for mRNA-reprogramming raises the question afterward whether the generated iPSCs are derived from reprogramming-mRNAs or positive effect of B-18-R-protein.

However, Warren et al. verified intracellular immune reactions only as per gene expression and not on the protein level. In contrast, we have searched for manifestation of an interferon immune response following mRNA transfection on the protein level, finding no increased levels of IFN-γ and -α as hallmarks of immune response in the supernatant of transfected cells. In our hands, applying B-18-R-protein, as a suppressor of type I interferon is not needed. We used *V. virus*-derived capping enzyme to insert non-modified natural cap 1 to 5′ end of RNA. Such system ensures 100% proper cap orientation for the resultant transcripts compared to cap analog ARCA where only ~80% of IVT-RNAs will be capped.

The proper capping of in vitro transcribed RNA (100% capping of transcripts) could contribute to mitigate immune response, and consequently reduce cytotoxicity. This could support repeated mRNA transfections for the iPS generation. However, the use of jetPEI (the effect of transfection reagent) itself might reduce cytotoxicity following mRNA transfection. We could confirm that jetPEI transfection could be used for mRNA-iPSCs generation with minimal cytotoxicity. We hypothesized that jetPEI itself might minimize cellular defensive actions following foreign nucleic acid transfection, and therefore minimize toxicity. As reported by a number of studies, application of some transfection reagents minimize cellular defensive actions following foreign nucleic acid transfection, and therefore minimize toxicity (Jensen et al., 2014).

4.7. Long-lasting reprogramming protein production

The short half-life of RNA molecules necessitates repeated transfections to generate mRNA-iPSCs. Thus, highly stable mRNA is desired to reduce transfection frequency. Especially the poly(A)tail length influences the stability of mRNA molecules and affects the translation. The subsequent addition of a poly(A)tail using a PolyA polymerase allows for tail lengths resembling the endogenous lengths of poly(A)tails of mRNAs in mammalian cells being approximately 200–300 adenosine residues long (Sheets & Wickens, 1989). This may allow for a higher stability of IVT-mRNAs compared to other reports (Warren et al., 2010) using shorter poly(A)tails of 120 residues. These reports also showed a reduction in expression of mRNA-introduced protein already 36 h after transfection, necessitating a daily transfection cycle (Warren et al., 2010; Mandal & Rossi, 2013). The long-lasting protein levels in our study enabled us to perform repeated transfection just every 48 h. The use of a cap1-structure naturally occurring in higher eukaryotic cells allows for a higher translation efficiency compared to cap analogs like ARCA resembling a cap0-structure.

Still, even while the transfection efficiency as well as the size of the mRNA molecules of the factors (OSKMN) was comparable, the protein levels of Klf4 and c-Myc were found to be higher compared to the other factors. The differences in the amount may be due to the different half-life times of the proteins.

The reported turnover times are highly variable, ranging from 24 h (Holt et al., 1996) to only 2.1 h for hTERT (Jung et al., 2013). While the half-life of c-Myc protein is considered to be short with about 20–30 min (Salghetti et al., 1999), it is known that especially under conditions like stress the half-life of c-Myc protein can increase (Alarcon-Vargas et al., 2002). The same is true for Nanog since several studies reported a half-life to be about 2 h (Ramakrishna et al., 2011; Chae et al., 2012; Abranches et al., 2013) while Filipczyk et al. measured a half-life of about 5.5 h (Filipczyk et al., 2013).

The percentages of GFP and hTERT positive cells were found to be lower compared to the other factors. This could be due to less efficient transfection of mRNA, (e.g. hTERT mRNA is larger than the other factor mRNAs) or due to a lower efficiency of protein translation.

4.8. Colony formation

The first sign of reprogramming was that the fibroblast morphology changed to a compact epithelioid morphology, indicative of MET (initiation phase of reprogramming). This is consistent with reports by other groups (Samavarchi-Tehrani et al., 2010; Li et al., 2010).

We could observe the first colony-like structures at day 8 compared to day 19 in the report by Rossi et al. (Warren et al., 2010). This might

have been due to the use of low oxygen, which has been reported to promote reprogramming (Utikal et al., 2009; Yoshida et al., 2009).

Nevertheless the efficiency of mRNA-reprogramming and the stability of generated colonies vary depending upon the origin, proliferative potential and genetic background of the fibroblasts. Taken together, the methodology we describe cuts mRNA reprogramming time.

Supplementary data to this article can be found online at http://dx.doi.org/10.1016/j.scr.2016.03.008.

Acknowledgments

References

Abranches, E., Bekman, E., Henrique, D., 2013. Generation and characterization of a novel mouse embryonic stem cell line with a dynamic reporter of Nanog expression. PLoS One 8, e59928.

Alarcon-Vargas, D., Tansey, W.P., Ronai, Z., 2002. Regulation of c-myc stability by selective stress conditions and by MEKK1 requires aa 127-189 of c-myc. Oncogene 21, 4384–4391.

Angel, M., Yanik, M.F., 2010. Innate immune suppression enables frequent transfection with RNA encoding reprogramming proteins. PLoS One 5, e11756.

Arnold, A., Naaldijk, M.Y., Fabian, C., et al., 2012. Reprogramming of human huntington fibroblasts using mRNA. ISRN Cell. Biol., 124878 http://dx.doi.org/10.5402/2012/124878 12 pp.

Bershteyn, M., Hayashi, Y., Desachy, G., Hsiao, E.C., Sami, S., Tsang, K.M., Weiss, L.A., Kriegstein, A.R., Yamanaka, S., Wynshaw-Boris, A., 2014. Cell-autonomous correction of ring chromosomes in human induced pluripotent stem cells. Nature 507, 99–103.

Chae, H.D., Lee, M.R., Broxmeyer, H.E., 2012. 5-Aminoimidazole-4-carboxyamide ribonucleoside induces G(1)/S arrest and Nanog downregulation via p53 and enhances erythroid differentiation. Stem Cells 30, 140–149.

Dressel, R., Guan, K., Nolte, J., et al., 2009. Multipotent adult germ-line stem cells, like other pluripotent stem cells, can be killed by cytotoxic T lymphocytes despite low expression of major histocompatibility complex class I molecules. Biol. Direct 4, 31.

Dressel, R., Nolte, J., Elsner, L., et al., 2010. Pluripotent stem cells are highly susceptible targets for syngeneic, allogeneic, and xenogeneic natural killer cells. FASEB J. 24, 2164–2177.

Drews, K., Tavernier, G., Demeester, J., et al., 2012. The cytotoxic and immunogenic hurdles associated with non-viral mRNA-mediated reprogramming of human fibroblasts. Biomaterials 33, 4059–4068.

Filipczyk, A., Gkatzis, K., Fu, J., et al., 2013. Biallelic expression of Nanog protein in mouse embryonic stem cells. Cell Stem Cell 13, 12–13.

Gore, A., Li, Z., Fung, H.L., et al., 2011. Somatic coding mutations in human induced pluripotent stem cells. Nature 471, 63–67.

Heng, B.C., Heinimann, K., Miny, P., et al., 2013. mRNA transfection-based, feeder-free, induced pluripotent stem cells derived from adipose tissue of a 50-year-old patient. Metab. Eng. 18, 9–24.

Holt, S.E., Wright, W.E., Shay, J.W., 1996. Regulation of telomerase activity in immortal cell lines. Mol. Cell. Biol. 16, 2932–2939.

Hou, P., Li, Y., Zhang, X., et al., 2013. Pluripotent stem cells induced from mouse somatic cells by small-molecule compounds. Science 341, 651–654.

Hussein, S.M., Batada, N.N., Vuoristo, S., et al., 2011. Copy number variation and selection during reprogramming to pluripotency. Nature 471, 58–62.

Jean, J.C., George, E., Kaestner, K.H., et al., 2013. Transcription factor Klf4, induced in the lung by oxygen at birth, regulates perinatal fibroblast and myofibroblast differentiation. PLoS One 8, e54806.

Jensen, K., Anderson, J.A., Glass, E.J., 2014. Comparison of small interfering RNA (siRNA) delivery into bovine monocyte-derived macrophages by transfection and electroporation. Vet. Immunol. Immunopathol.

Jia, F., Wilson, K.D., Sun, N., et al., 2010. A nonviral minicircle vector for deriving human iPS cells. Nat. Methods 7, 197–199.

Jung, H.Y., Wang, X., Jun, S., et al., 2013. Dyrk2-associated EDD-DDB1-VprBP E3 ligase inhibits telomerase by TERT degradation. J. Biol. Chem. 288, 7252–7262.

Karikó, K., Weissman, D., 2007. Naturally occurring nucleoside modifications suppress the immunostimulatory activity of RNA: implication for therapeutic RNA development. Curr. Opin. Drug Discov. Devel. 10, 523–532.

Karikó, K., Buckstein, M., Ni, H., et al., 2005. Suppression of RNA recognition by toll-like receptors: the impact of nucleoside modification and the evolutionary origin of RNA. Immunity 23, 165–175.

Karikó, K., Muramatsu, H., Welsh, F.A., et al., 2008. Incorporation of pseudouridine into mRNA yields superior nonimmunogenic vector with increased translational capacity and biological stability. Mol. Ther. 16, 1833–1840.

Kim, T., Bershteyn, M., Wynshaw-Boris, A., 2014. Chromosome therapy: correction of large chromosomal aberrations by inducing ring chromosomes in induced pluripotent stem cells (iPSCs). Nucleus 5, 391–395.

Kuge, H., Brownlee, G.G., Gershon, P.D., et al., 1998. Cap ribose methylation of c-mos mRNA stimulates translation and oocyte maturation in *Xenopus laevis*. Nucleic Acids Res. 26, 3208–3214.

Li, R., Liang, J., Ni, S., et al., 2010. A mesenchymal-to-epithelial transition initiates and is required for the nuclear reprogramming of mouse fibroblasts. Cell Stem Cell 7, 51–63.

Lister, R., Pelizzola, M., Kida, Y.S., et al., 2011. Hotspots of aberrant epigenomic reprogramming in human induced pluripotent stem cells. Nature 471, 68–73.

Mah, N., Wang, Y., Liao, M.C., Prigione, A., Jozefczuk, J., Lichtner, B., Wolfrum, K., Haltmeier, M., Flöttmann, M., Schaefer, M., Hahn, A., Mrowka, R., Klipp, E., Andrade-Navarro, M.A., Adjaye, J., 2011. Molecular insights into reprogramming-initiation events mediated by the OSKM gene regulatory network. PLoS One 6, e24351.

Mandal, P.K., Rossi, D.J., 2013. Reprogramming human fibroblasts to pluripotency using modified mRNA. Nat. Protoc. 8, 568–582.

Mayshar, Y., Ben-David, U., Lavon, N., et al., 2010. Identification and classification of chromosomal aberrations in human induced pluripotent stem cells. Cell Stem Cell 7, 521–531.

Navarro, A., Rezaiekhaligh, M., Keightley, J.A., et al., 2009. Higher TRIP-1 level explains diminished collagen contraction ability of fetal versus adult fibroblasts. Am. J. Phys. Lung Cell. Mol. Phys. 296, L928–L935.

Plews, J.R., Li, J., Jones, M., et al., 2010. Activation of pluripotency genes in human fibroblast cells by a novel mRNA based approach. PLoS One 5, e14397.

Ramakrishna, S., Suresh, B., Lim, K.H., et al., 2011. PEST motif sequence regulating human NANOG for proteasomal degradation. Stem Cells Dev. 20, 1511–1519.

Robinton, D.A., Daley, G.Q., 2012. The promise of induced pluripotent stem cells in research and therapy. Nature 481, 295–305.

Salghetti, S.E., Kim, S.Y., Tansey, W.P., 1999. Destruction of Myc by ubiquitin-mediated proteolysis: cancer-associated and transforming mutations stabilize Myc. EMBO J. 18, 717–726.

Samavarchi-Tehrani, P., Golipour, A., David, L., et al., 2010. Functional genomics reveals a BMP-driven mesenchymal-to-epithelial transition in the initiation of somatic cell reprogramming. Cell Stem Cell 7, 64–77.

Sheets, M.D., Wickens, M., 1989. Two phases in the addition of a poly(A) tail. Genes Dev. 3, 1401–1412.

Shields, J.M., Christy, R.J., Yang, V.W., 1996. Identification and characterization of a gene encoding a gut-enriched Krüppel-like factor expressed during growth arrest. J. Biol. Chem. 271, 20009–20017.

Silva, J., Nichols, J., Theunissen, T.W., Guo, G., van Oosten, A.L., Barrandon, O., Wray, J., Yamanaka, S., Chambers, I., Smith, A., 2009. Nanog is the gateway to the pluripotent ground state. Cell 138, 722–737.

Stadtfeld, M., Nagaya, M., Utikal, J., et al., 2008. Induced pluripotent stem cells generated without viral integration. Science 322, 945–949.

Taapken, S.M., Nisler, B.S., Newton, M.A., et al., 2011. Karotypic abnormalities in human induced pluripotent stem cells and embryonic stem cells. Nat. Biotechnol. 29, 313–314.

Takahashi, K., Yamanaka, S., 2006. Induction of pluripotent stem cells from mouse embryonic and adult fibroblast cultures by defined factors. Cell 126, 663–676.

Takahashi, K., Tanabe, K., Ohnuki, M., et al., 2007. Induction of pluripotent stem cells from adult human fibroblasts by defined factors. Cell 131, 861–872.

Tang, G.Q., Bandwar, R.P., Patel, S.S., 2005. Extended upstream A-T sequence increases T7 promoter strength. J. Biol. Chem. 280, 40707–40713.

Tavernier, G., Wolfrum, K., Demeester, J., et al., 2012. Activation of pluripotency-associated genes in mouse embryonic fibroblasts by non-viral transfection with in vitro-derived mRNAs encoding Oct4, Sox2, Klf4 and cMyc. Biomaterials 33, 412–417.

Theunissen, T.W., van Oosten, A.L., Castelo-Branco, G., Hall, J., Smith, A., Silva, J.C., 2011. Nanog overcomes reprogramming barriers and induces pluripotency in minimal conditions. Curr. Biol. 21, 65–71.

Utikal, J., Polo, J.M., Stadtfeld, M., et al., 2009. Immortalization eliminates a roadblock during cellular reprogramming into iPS cells. Nature 460, 1145–1148.

Warren, L., Manos, P.D., Ahfeldt, T., et al., 2010. Highly efficient reprogramming to pluripotency and directed differentiation of human cells with synthetic modified mRNA. Cell Stem Cell 7, 618–630.

Warren, L., Ni, Y., Wang, J., et al., 2012. Feeder-free derivation of human induced pluripotent stem cells with messenger RNA. Sci. Report. 2, 657.

Wirth, H., Löffler, M., von Bergen, M., et al., 2011. Expression cartography of human tissues using self organizing maps. BMC Bioinform. 12, 306.

Wirth, H., von Bergen, M., Binder, H., 2012. Mining SOM expression portraits: feature selection and integrating concepts of molecular function. BioData Min. 5, 18.

Yakubov, E., Rechavi, G., Rozenblatt, S., et al., 2010. Reprogramming of human fibroblasts to pluripotent stem cells using mRNA of four transcription factors. Biochem. Biophys. Res. Commun. 394, 189–193.

Yoshida, Y., Takahashi, K., Okita, K., et al., 2009. Hypoxia enhances the generation of induced pluripotent stem cells. Cell Stem Cell 5, 237–241.

Yoshioka, N., Gros, E., Li, H.R., Kumar, S., Deacon, D.C., Maron, C., Muotri, A.R., Chi, N.C., Fu, X.D., Yu, B.D., Dowdy, S.F., 2013. Efficient generation of human iPSCs by a synthetic self-replicative RNA. Cell Stem Cell 13, 246–254.

Yu, J., Hu, K., Smuga-Otto, K., et al., 2009. Human induced pluripotent stem cells free of vector and transgene sequences. Science 324, 797–801.

Yusa, K., Rad, R., Takeda, J., et al., 2009. Generation of transgene-free induced pluripotent mouse stem cells by the piggyBac transposon. Nat. Methods 6, 363–369.

Zhou, Y.Y., Zeng, F., 2013. Integration-free methods for generating induced pluripotent stem cells. Genomics Proteomics Bioinformatics 11, 284–287.